

Response to Referee #3

Warm protons at comet 67P/Churyumov-Gerasimenko – Implications for the infant bow shock

We thank the referee for the constructive comments and suggestions. We have made the necessary amendments to the paper and answers to comments may be found below. (Blue: Referee comment, black: our answer).

Near Line 70, in this paper you are mainly exploring the characteristics in the data when the spacecraft crossed the infant shock. Can you also briefly mention and cite some references on what the data will be like if an ordinary or classical shock is crossed, so that readers can easily see the similarities and differences between the infant shock and the ordinary shock. It becomes clear now that the short introduction into the topic of classical bow shocks is not extensive enough. Therefore we added a more detailed summary of this topic.

Line 159 & 160: "Interestingly, the flux diminishes at the same time that the proton energy increases gradually." Can you add some theoretical explanation to this phenomena?

A detailed theoretical explanation will be quite difficult, but something similar was already observed by Gunell et al (2018). We think that the spacecraft is slowly transitioning into a different region behind the IBS, just as observed in the first event described by Gunell et al (2018). We have added a reference to this in the text.

Line 163: the angle between the x-axis and magnetic field -¿ the angle between the x-axis and electric field?

Both of these are correct, because we estimate the electric field from the magnetic field. The electric field is the more physically relevant parameter, so we have changed it in the text.

Line 166: Does spacecraft attitude mean spacecraft orientation? Can you explain what are $\alpha_{x,y,z}$ of the spacecraft attitude?

Yes, spacecraft attitude means the orientation of the spacecraft in a certain frame of reference. $\alpha_{x,y,z}$ are the angles of the spacecraft axes (x, y, z) to the Comet-Sun line. However, we have since removed the spacecraft attitude from these figures as it provided little information. Instead we added in the Data Section that events with attitude changes above $> 10^\circ$ were discarded.

Line 173: "we find that the energy of the electrons is almost always increased". Is it consistent with your expectations? Can you add explanation the increase of electron energy and decrease in ion energy?

It is indeed consistent with expectations. In this section we limit ourselves to the description of the data analysis, the discussion is done in the later section, where the text addresses this finding.

Line 244: The statement "at least some of this discrepancy might be attributable to the inability of the flux at 60eV or 120eV to accurately represent the electron spectra" is not clear to me. Can you elaborate this point?

The electron flux measured by IES depends on the FOV of the instrument as well as the spacecraft charge. Depending on these parameters, the measured flux will deviate significantly from the true state of the plasma, and this is of course also reflected in the flux at these specific two energies. A clarification that relates this back to the instrument caveats in section 2.1 was added.

Line 2: after "infant bow shock" add "(IBS)".

Line 25: "and with it the amount of ice" -¿ "with increasing amount of ice"

Line 40: lower gyroradii -¿ smaller gyroradii

Line 49: "the comet's, frame of reference" -¿ "the comet's frame of reference"

Line 66: "insure" -¿ "ensure"

Line 74: "it's characteristics" -¿ "its characteristics"

Line 119: "instead" -¿ "because" ?

Line 138: by-eye inspection -¿ inspection by eyeball ?

Line 201: below than above unity -¿ below unity?
All these typos have been corrected.

Significant Text Changes

~~Multiple plasma boundaries have been observed at~~ The plasma around comet 67P/Churyumov-Gerasimenko ~~Among them was an~~ shows remarkable variability throughout the entire Rosetta mission. Plasma boundaries such as the diamagnetic cavity, solar wind ion cavity and infant bow shock ~~, an asymmetric structure separate regions with distinct plasma parameters from each other. Here, we focus on a particular feature in the plasma environment that separates the less disturbed solar wind from a plasma with warmer, slower protons. Rosetta crossings of the infant bow shock have so far only been reported for two days. Here, we aim to investigate this phenomenon: warm, slow solar wind protons. We investigate this particular proton population further by focusing on the proton behaviour and surveying all of the Rosetta comet phase data. We find over 300 events that match the proton signatures at the infant bow shock ~~where Rosetta transitted from a region with fast, cold protons into a region with warm, slow protons.~~~~

~~Both~~ These results agree well with simulations of the infant bow shock (IBS), an asymmetric structure in the plasma environment previously detected on only two days during the comet phase. The properties of the plasma on both sides of this structure.

As a comet approaches the Sun, energy input into the surface increases ~~and with it~~ which increases the amount of ice that is sublimated and escapes into space.

At higher gas production rates this asymmetry is less pronounced and the influence of the cometary ion gyroradius is diminished, because the magnetic field pile-up at the comet results in higher field magnitudes and thus ~~lower gyroradii~~ smaller gyroradii.

Boundaries in the plasma at 67P have been identified and characterized in many publications. The three main boundaries that were observable by Rosetta were, in order of decreasing cometocentric distance, the solar wind ion cavity (e.g. Nilsson et al., 2017), a collisionopause (Mandt et al., 2016), and the diamagnetic cavity (e.g. Goetz et al., 2016a,b). The solar wind ion cavity is the region where no solar wind ions can be observed in the plasma, from May 2015 to January 2016 Rosetta was almost exclusively within this region. The collisionopause demarcates the tenuous boundary where ion-neutral or electron-neutral collisions become important and it has been shown to lie within the solar wind ion cavity. Finally the diamagnetic cavity is the innermost observed region, where the magnetic field is very close to zero. For a more detailed overview of these boundaries see e.g. Götz et al. (2019).

Another boundary in the plasma environment of a comet, but not observed by Rosetta, is the bow shock.

There, the interaction between the solar wind and the comet cannot be described by mass-loading alone, instead the flow changes from supersonic to subsonic and a bow shock forms. This prediction is shown to fit well with observations at e. g. comet Halley (Neubauer et al., 1986), where the bow shock was detected 1.15×10^6 km from the nucleus. The transition from unshocked to shocked solar wind was identified by a decrease in speed, increase in density and temperature and an increase in the magnetic field (Coates et al., 1990). The shock was identified as a low Mach number shock, in agreement with the model, which predicted a gradual slowing of the solar wind flow already upstream of the shock due to the incorporation of the cometary ions. The cometary ion density is often neglected in bow shock models at high activity comets, because it only reaches 1.5-2.5% of the total density. Observations of bow shocks at other comets where quite similar, although at the lower activity comets Giacobini-Zinner (GZ) and Grigg-Skjellerup (GS) the bow shock is often termed a bow wave, due to the lack of a sharp boundary (Smith et al., 1986). At GS, a strong non-gyrotropy of the cometary ions could be observed near the bow wave, together with wave activity triggered by this unstable distribution function (Coates et al., 1996). Koenders et al. (2013) compare the bow shock distances from a simple single-fluid model with distances gained from Hybrid simulations and find that the fluid models predicted consistently higher stand off distances. Thus, the ion gyroradius effects are pronounced even in the most fluid-like stage of the plasma around comet 67P. ~~The shock~~

The shock itself forms by waves steepening into the nonlinear regime. The speed of the steepened wave is faster than that of the linear wave, but steepening is counteracted by dissipation. If an obstacle and a plasma are in relative motion faster than the speed of linear waves, the waves steepen until an equilibrium is reached where the shock becomes a stationary wave in the obstacle, ~~in this case~~ s (the comet's, ~~)~~ frame of reference (Balogh and Treumann, 2013).

~~Koenders et al. (2013) compare the bow shock distances from a simple single-fluid model with distances gained from Hybrid simulations and find that the fluid models predicted consistently higher stand off distances. Thus, the ion gyroradius effects are pronounced even in the most fluid-like stage of the plasma around comet 67P.~~

According to Balogh and Treumann (2013), the slowing down and heating of the medium over a narrow layer or boundary is the defining feature of any shock.

Often, the signal is then still visible in the RPC-IES instrument, as the FOV is partially complimentary (rotated by 60°), a detailed description of the FoV can be found in the ICA User Guide on the PSA¹. Solar wind

¹<https://cosmos.esa.int/web/psa/rosetta>

Start time	H ⁺ E/q	$\Gamma_{IES,e}$	B_m	P_B	$\cos(\theta)$	$V_{s/c} n_{pl}$	T_p	H ⁺ E/q	$\Gamma_{IES,e}$	B_m	P_B	$\cos(\theta)$	$V_{s/c}$
Dec 07, 14 03:49	↓	↑	~	↓	-	-	↑	↑	-	-	-	-	-
Dec 25, 14 09:50	↓	↑	↓	↓	-	-	↑	↑	↓	-	-	-	-
Jan 04, 15 12:19	↓	↑	-	↓	-	-	↑	↑	-	-	↑	-	-
Jan 04, 15 19:55	↓	↑	↑	-	-	-	~	↑	↓	↑	-	↓	-
Mar 07, 15 05:48	↓	↑	↑	↑	↑	-	↓	↑	↓	↓	-	↓	-
Feb 10, 16 09:02								↑	↓	↓	↓	↓	↓
Feb 26, 16 05:50	↓	-	-	-	-	-	~	↑	-	↓	-	↓	↓
Feb 29, 16 00:27	↓	-	-	-	↓	-	~	↑	↓	↓	↓	↑	-
Apr 08, 16 03:27	↓	↑	↓	↓	↑	↑	~	↑	↓	↑	↑	↓	↓
Apr 08, 16 07:58	↓	↑	↓	↑	-	↑	~	↑	↓	↑	-	↓	↓
Jun 01, 16 12:11	↓	↑	↑	↑	↑	↑	↑	↑					
Jul 09, 16 12:43	↓	↑	↑	↑	-	↑	↑	↑	↓	-	-	↓	-
Jul 09, 16 15:52	↓	↑	↓	↓	-	↑	↑	↑	↓	-	-	↑	-
Median	↓	↑	-	-	-	-↑	↑	↑	↓	-	-	↓	-

Table 1: List of 13 events chosen for a more detailed study and list of parameter changes when crossing from upstream to downstream (inward, left) and from downstream to upstream (outward, right). The last line summarizes events by giving a median change. Missing signs indicate that no data was available.

densities near the comet also decrease due to significant charge exchange losses (Simon Wedlund et al., 2019). This caused rather low densities in the times when Rosetta was just outside the solar wind ion cavity. The RPC-ICA ~~moments~~ solar wind moments, including the temperature, used in this study are integrations of the RPC-ICA PSA L4 PHYS-MASS data set, also delivered to the planetary science archive (PSA) as RPC-ICA L5 MOMENT data set. ~~We chose to use the mean proton speed $v_{m,H}$ derived from this data set for assessment of the speed near the IBS. This value is derived by calculating the mean velocity of the proton energy distribution and thus is a more suitable parameter than the 3D velocity moment which is heavily influenced by the pitch angle distribution of the protons (Behar et al., 2017). Here, we only use values for which the density of the protons (calculated from the flux) is above 0.005 cm^{-3} which is the case for about 90% of all values.~~

~~Its FoV is partially complementary to ICA, but the The time resolution is at least 256 s. The, and the measurements at low energies are disturbed by the spacecraft potential, which is between 0 V and -20 V most of the time.~~

~~(Johansson et al., 2020). For this study, we use the density estimate to characterize the plasma.~~

~~These are the two criteria used~~ For the first criterion, the threshold was a shift of the peak of the ion spectra by at least three energy bins, corresponding to at least 60 eV. We only use these two criteria for detection. For verification we evaluate additional properties like the ICA derived proton temperature, plasma density, suprathermal electron fluxes, magnetic field magnitude power spectral density in the frequency range between 50 mHz and 75 mHz and the magnetic field magnitude. However, the direction of change (increase or decrease) is not considered, ~~instead because~~ the change in parameters is simply an indicator that the change in proton energy and flux is not due to instrumental or spacecraft effects.

We also use the sun aspect angles of the spacecraft to exclude an attitude change of the spacecraft as a reason for a change in the proton signal. These are defined as the angles of the three spacecraft axes to the Sun-comet line². Events that coincide with major attitude changes ($> 10^\circ$) are not included in the study.

Other parameter changes like solar wind velocity and density as well as cometary ion density can also ~~cause move the boundary, causing~~ warm protons to appear ~~(as stated in previous publications)~~ at the spacecraft ~~(as stated in Gunell et al., 2018)~~.

The He^+ and He^{2+} show a very similar behaviour to the protons (panel a), decreasing and broadening in energy, but their signature remains distinct from each other at all times. The IES electron signature (panel d) increases in energy and flux. Interestingly, the flux diminishes at the same time that the proton energy increases gradually~~, implying that the spacecraft moved slowly upstream in a shock-fixed frame of reference into a region with less electron heating and a less slowed-down proton distribution. This is similar to what was observed already by Gunell et al. (2018)~~.

This is because θ represents the angle between the x-axis and ~~magnetic electric~~ field, thus it does not reflect changes in the z-component of the magnetic field very well. The ~~spacecraft potential plasma density~~ (panel h) ~~is lower in the downstream region. We use this as a proxy for the density of the plasma: the lower the spacecraft potential, the higher the density. Thus the density is higher in the downstream region. We also ensure that these changes in the particle signatures are not due to a change in FoV, thus we included the spacecraft attitude as well as the proton temperature~~ (panel i) ~~to confirm that it only changes insignificantly in the time interval~~

²See <https://www.cosmos.esa.int/web/spice/spice-for-rosetta>

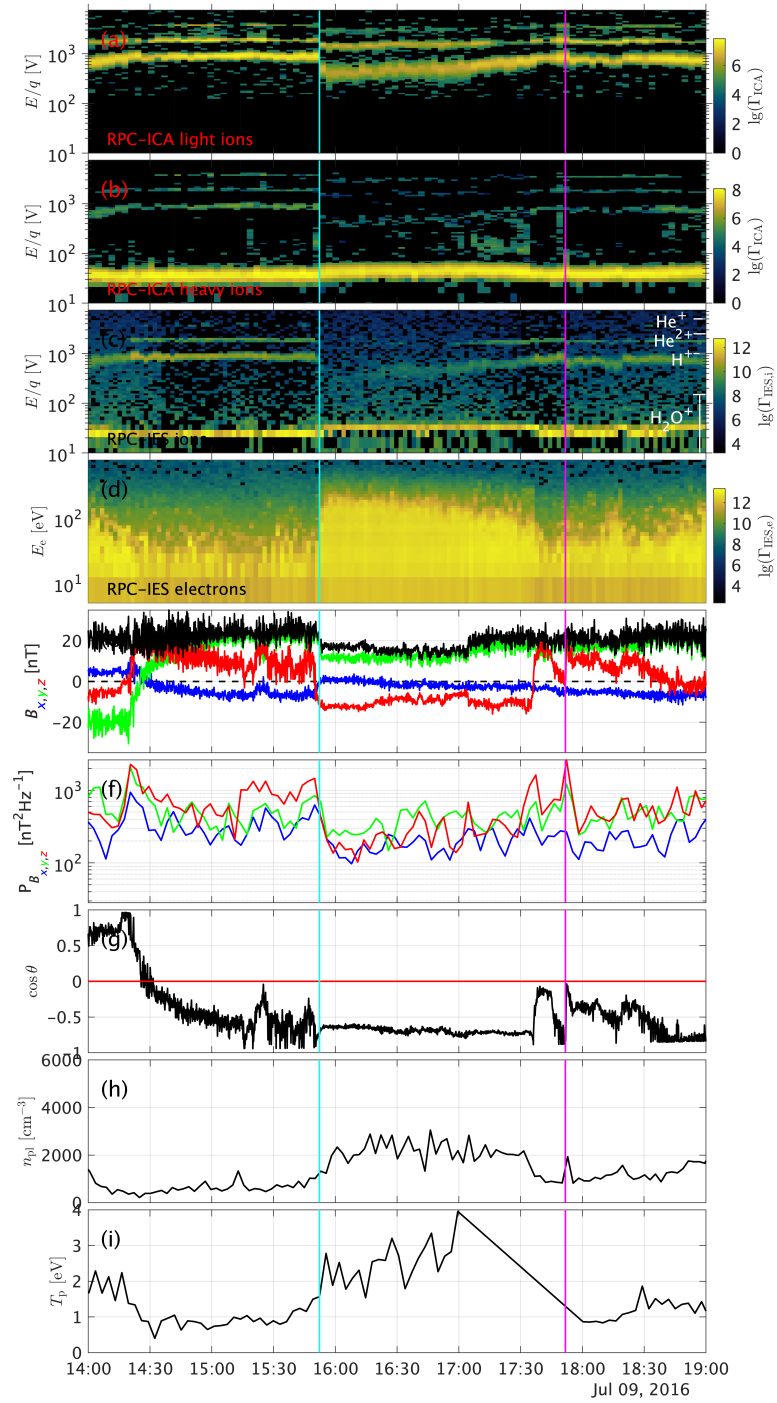


Figure 1: Observations of the event on July 9th, 2016. From top to bottom: a) ICA solar wind ions, b) ICA heavy ions, c) IES ions, d) IES electrons, e) magnetic field in CSEQ coordinates, f) magnetic power spectral density in the frequency range between 2 mHz and 15 mHz, g) angle between spacecraft position and convective electric field, h) spacecraft potential plasma density from LAP, and i) attitude ID proton temperature from ICA.

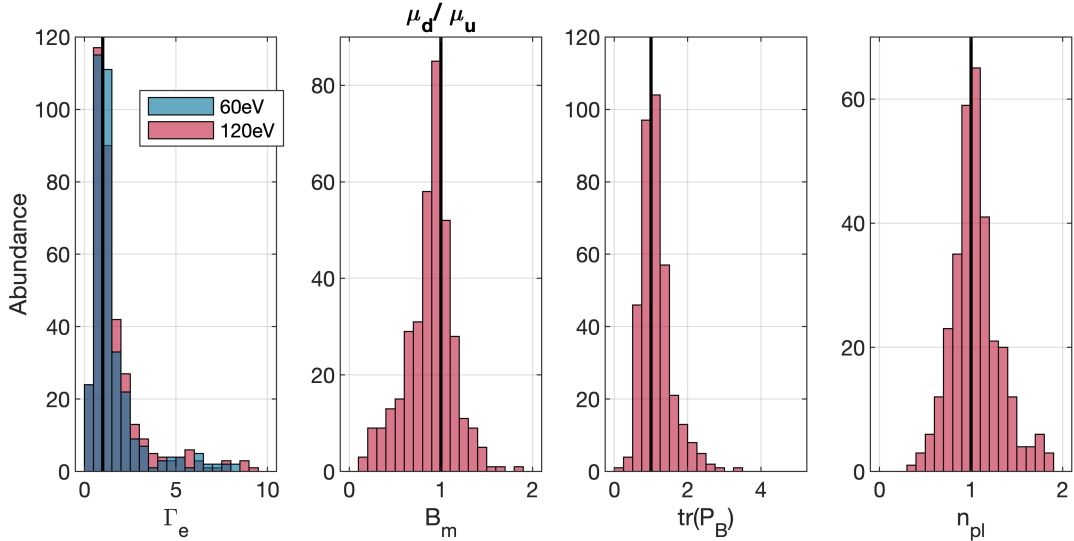


Figure 2: Comparison of the upstream and downstream mean values for ~~five-four~~ of the ~~six-seven~~ parameters chosen for investigation. From left to right: Electron flux Γ_e at 60 eV (blue) and at 120 eV (red), magnetic field strength B_m , trace of the magnetic field power spectral density $\text{tr}(P_B)$, and plasma density n_{pl} .

~~in question are higher in the downstream region.~~

The parameters that we use to characterize how the plasma changes at the boundary are the proton energy $H^+ E/q$, the flux of the electrons $\Gamma_{IES,e}$, the magnetic field magnitude B_m , the power spectral density of the magnetic field P_B , the angle $\cos(\theta)$, ~~and the spacecraft potential $V_{s/c}$, the plasma density n_{pl} , and the proton temperature T_p .~~ The changes are indicated in Table 1. Here, we are only looking at the qualitative changes, quantitative changes will be assessed in the next section, where the larger statistics should make up for the large uncertainty for each event. These clear, qualitative events can then be used to verify the quantitative, statistical outcome.

From these events we can conclude: Since the proton energy was used as a selection criterion the proton energy in the downstream region is always lower than upstream. The proton temperature is almost always higher in the downstream region. For the other parameters, we find that the energy of the electrons is almost always increased and the ~~spacecraft potential is often lower~~ density is often higher in the downstream region.

The statistical assessment of the proton flux is complicated by an incomplete FoV and the broad distribution of the protons. Therefore, moments of the distribution function are less representative in the situation at comet 67P. ~~Instead, we use the mean speed of the protons: a simple 1D approximation of the energy spectra of the protons. This parameter does not represent the angular spread of the particles, but it is the most representative of the energy vs. time spectrograms that we used to identify events. Even this parameter is not always reliable, as it only uses ICA spectra and some events that were identified earlier are only (better) visible in the IES spectra. Therefore a direct statistical study of the moments cannot be conducted.~~ To assess the electron flux changes, we chose two energy values (60 eV and 120 eV) to extract a 1D time series of the flux at these energies. They were chosen based on an inspection of the subset of events, ~~were where~~ these energy bands showed the clearest change.

These larger statistics agree mostly with the observations from the 13 events that were categorized by hand. From left to right:

~~$v_{m,H}$ The proton energy (decrease) and width of the energy spectra (increase) were originally chosen as selection criteria. The downstream to upstream ratio shows a larger number of values below than above unity as expected for a decrease in energy as was seen in Sect. ???. However, the mean speed of the protons does not always decrease. This is probably due to the way that the mean speed is calculated, as it is the centre of weight of the energy spectra. For a low signal-to-noise ratio, this value is not meaningful.~~

Γ_e In our smaller subset, the energy of the electrons in the 60 eV and 120 eV band increases in 10 of the 12 inbound passes and decreases in 8 of the 12 outbound passes. In the entire dataset the electron energy is increased in the downstream region in 60% of all cases. That the larger statistics do not show the same behaviour may in part be because the energy dependent electron flux is difficult to condense to a single parameter, and the instrument sensitivity declined significantly after perihelion. We have observed cases ~~where~~ where the flux was very low and thus changes were not visible.

B_m The magnetic field decreases in 68% of cases. This is consistent with the case studies above.

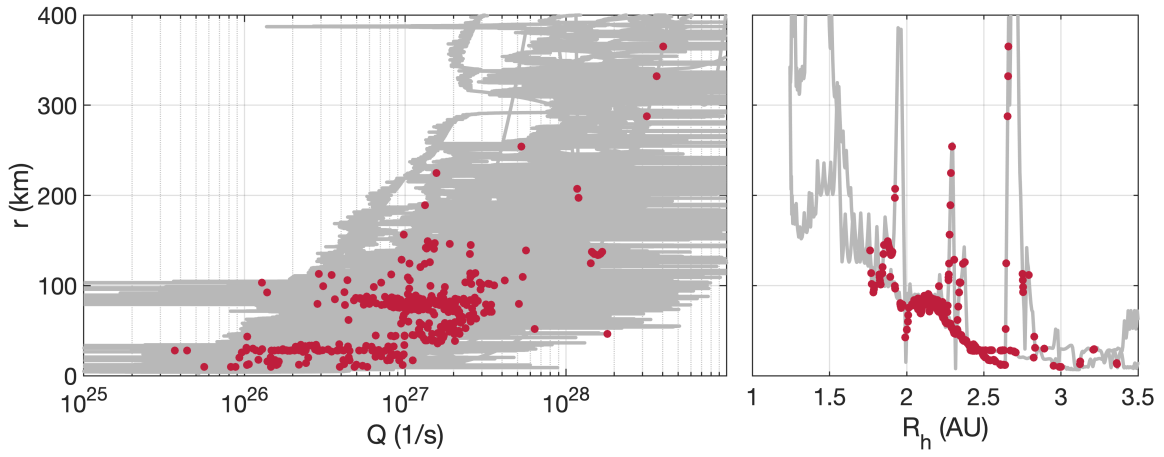


Figure 3: Cometocentric distance of the spacecraft over gas production rate (left) and heliocentric distance (right). The gas production rate was derived from measured neutral gas densities using a spherically symmetric model. The grey lines show the position during the entire Rosetta mission, while the red dots indicate boundary crossings.

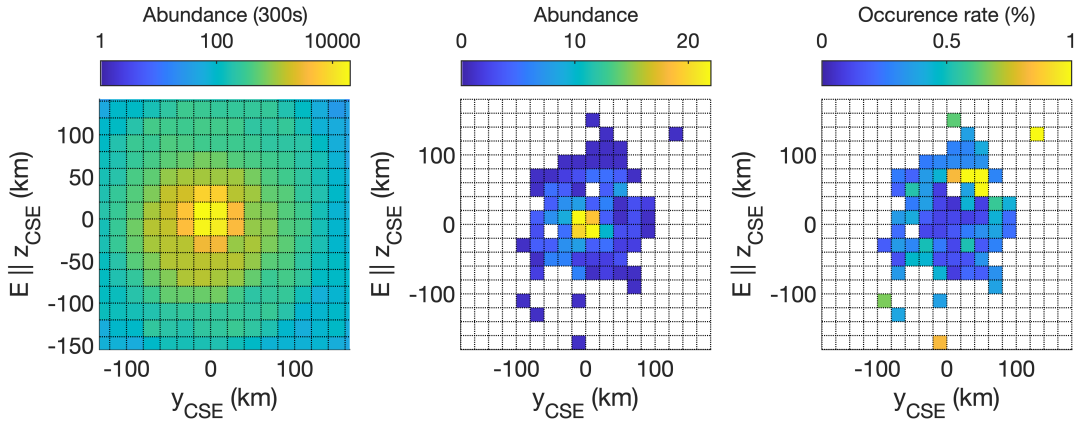


Figure 4: Abundance of the position of the spacecraft (left), position at which warm protons were detected (middle) and occurrence rate of detections normalized to the spacecraft dwell time (right). The $+E_c$ hemisphere is that of $z_{CSE} \geq 0$.

$\text{tr}(P_B)$ The trace power spectral density increases downstream in 58% of all cases.

~~U_{sc} The spacecraft potential decreases~~

n_{pl} The plasma density increases in 52% of all cases. This is consistent with the case studies, where the ~~spacecraft potential was either decreased~~ density was either increased downstream or not changed at all.

The relevant gyroperiods of 0.5 s (protons) and 9 s (water ions) are much smaller than any of the transition times we observe. The behaviour of the magnetic field magnitude is an example of this. In shock modelling, the magnetic field is generally stronger on the downstream than the upstream side of the shock. In our statistics, we have many cases of the opposite behaviour. One possibility is that an increase in the solar wind dynamic pressure pushes the increases the mass-loading threshold of the plasma (Biermann et al., 1967) which means that the critical condition for a shock is met later in the flow, and thus closer to the comet. This moves the IBS further towards the ~~comet nucleus~~ and Rosetta passes into the upstream region, but at the same time the magnitude of the interplanetary field increases, resulting in a new, stronger magnetic field.

DIFdelbegin ~~When considering~~ We can also consider just the subset of events where the plasma behaves as expected for an IBS (the magnetic field increases downstream along with an increase in the power spectral density, increase in electron flux). ~~About 10% of all events fulfil all these criteria and one~~ In about 10% of the cases all parameters that were evaluated, the magnetic field included, behave as expected at the same time. One such event is shown in Fig. ???. Although the ICA data is missing for the first half of the event (before 06:30), we can clearly see warm proton fluxes in the IES data ~~for the first half of the event. For the second half~~

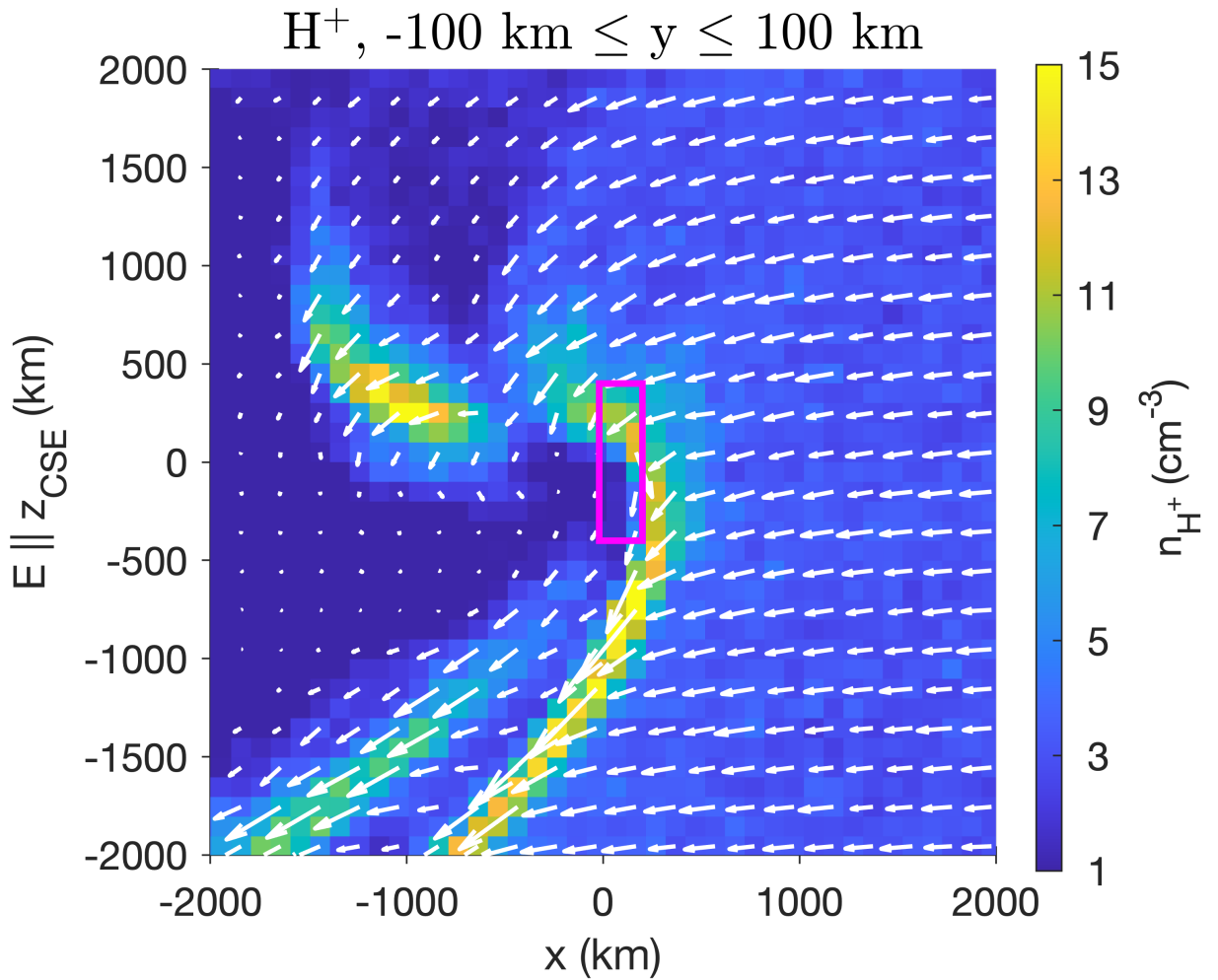


Figure 5: Density and direction of the flux of the protons from the Hybrid simulations. [The simulation was run for a case of \$Q = 3.2 \times 10^{27} \text{ s}^{-1}\$. For a more detailed list of parameters see \[Gunell et al. \\(2018\\)\]\(#\).](#) Here, the Sun is to the right. [The IBS is roughly located where the proton density reaches its highest values \(yellow\).](#)

~~they are registered by ICA while ICA is off. Once ICA is running, the protons do appear in the ICA energy spectra.~~

We present here also for the first time the ~~spacecraft potential~~ plasma density measurements for this boundary. We find that the ~~spacecraft potential, and by extension the~~ density of the plasma on average does not change significantly at the boundary. ~~In fact, events where the plasma density increases, decreases and is unchanged can all be found in the data set.~~ This was expected, as the plasma density at 67P at this point is dominated by the heavy ions and not the solar wind. ~~Thus, the~~ We can estimate the fraction of cometary ions for the event shown in Fig. 1. The cometary ion density is of the order of 1000 cm^{-3} and we can estimate the maximum proton density from a simple back-of-the-envelope calculation: assuming a solar wind density of 3 cm^{-3} (typical for heliocentric distances around 2 AU) and a compression factor of ~ 4 , we get a proton density of 12 cm^{-3} . This is close to what is also observed in the simulation used below. This gives a fraction of $\sim 99\%$ cometary ions. Even if this estimate is very rough, it is clear that the cometary ions are at this point clearly dominating the plasma density and the solar wind has only very little influence ~~on the plasma density~~ density-wise. Instead ? found that the solar wind and cometary ion momentum are of similar importance at the intermediate stage of cometary activity.

The gyroradii of protons in the $200 - 400\text{ km s}^{-1}$ range are $100 - 200\text{ km}$ in a 20 nT magnetic field. This is comparable to the thickness of the infant bow shock. The typical length scale of the structure in the upper left corner of Fig. 5 is about 10^3 km , corresponding to approximately 2 gyroradii in the weaker magnetic field ($\sim 10\text{ nT}$) in that region.

~~We have made attempts to conclusively show that this structure is indeed a shock in the fluid dynamics sense~~ In order to provide proof that a boundary in a plasma is a shock, usually Rankine-Hugoniot are evaluated. However, the plasma environment of the comet is far from a single fluid MHD plasma where the Rankine-Hugoniot R-H conditions could be used to investigate the transition. ~~Such an approach has been employed in the past in the analysis of the Giotto flybys of comets 1P/Halley and 26P/Grigg-Skjellerup (Coates et al., 1990, 1997).~~ Kessel et al. (1994) expanded the fluid theory to include effects of multiple ion species. For our situation, multi-ion and kinetic scale effects ~~need to~~, and the non-stationarity of the shock ~~need~~ be accounted for.

Omidi and Winske (1987) conducted one-dimensional hybrid simulations with the aim of modelling the spacecraft encounters with comets 1P/Halley and 21P/Giacobini-Zinner. They found that for oblique interaction (cone angle 55°), shocklets form in a region of large amplitude wave activity. These shocklets convect downstream, where they break up due to dispersion, and new ones form further upstream. Thus, the process is repeated in a way that resembles shock reformation at planets (e.g. Balogh and Treumann, 2013). Although it is possible that shocklets form and shock reformation occurs also at comet 67P under certain conditions, it is not the cause of the observations reported here. The shock encounters shown in Figs. 1, ??, 6, and 7 do not display the repetitive transitions in a wave-dominated region that would be expected for the shocklets reported by Omidi and Winske (1987).

It ~~is~~ ~~may be that~~ the infant bow shock ~~that develops into the ordinary~~ is the low gas production rate manifestation of what becomes the more developed cometary bow shock as ~~the comet moves closer to the Sun and the outgassing increases further~~ observed at larger comets such as Halley.

References

- André Balogh and Rudolf A. Treumann. *Physics of Collisionless Shocks*, volume 12 of *ISSI Scientific Report Series*. Springer, New York, NY, 2013. ISBN 978-1-4614-6099-2. doi: 10.1007/978-1-4614-6099-2.
- E. Behar, H. Nilsson, M. Alho, C. Goetz, and B. Tsurutani. The birth and growth of a solar wind cavity around a comet - Rosetta observations. *MNRAS*, 469:S396–S403, July 2017. doi: 10.1093/mnras/stx1871.
- L. Biermann, B. Brosowski, and H. U. Schmidt. The interactions of the solar wind with a comet. *Solar Physics*, 1:254–284, March 1967. doi: 10.1007/BF00150860.
- A. J. Coates, A. D. Johnstone, R. L. Kessel, D. E. Huddleston, and B. Wilken. Plasma parameters near the comet Halley bow shock. *J. Geophys. Res.*, 95:20701–20716, December 1990. doi: 10.1029/JA095iA12p20701.
- A. J. Coates, A. D. Johnstone, and F. M. Neubauer. Cometary ion pressure anisotropies at comets Halley and Grigg-Skjellerup. *J. Geophys. Res.*, 101(A12):27573–27584, December 1996. doi: 10.1029/96JA02524.
- A. J. Coates, C. Mazelle, and F. M. Neubauer. Bow shock analysis at comets Halley and Grigg-Skjellerup. *J. Geophys. Res.*, 102(A4):7105–7113, April 1997. doi: 10.1029/96JA04002.
- C. Goetz, C. Koenders, K. C. Hansen, J. Burch, C. Carr, A. Eriksson, D. Frühauff, C. Güttler, P. Henri, H. Nilsson, I. Richter, M. Rubin, H. Sierks, B. Tsurutani, M. Volwerk, and K. H. Glassmeier. Structure and evolution of the diamagnetic cavity at comet 67P/Churyumov-Gerasimenko. *MNRAS*, 462:S459–S467, November 2016a. doi: 10.1093/mnras/stw3148.

- C. Goetz, C. Koenders, I. Richter, K. Altwegg, J. Burch, C. Carr, E. Cupido, A. Eriksson, C. Güttler, P. Henri, P. Mokashi, Z. Nemeth, H. Nilsson, M. Rubin, H. Sierks, B. Tsurutani, C. Vallat, M. Volwerk, and K.-H. Glassmeier. First detection of a diamagnetic cavity at comet 67P/Churyumov-Gerasimenko. *A&A*, 588:A24, April 2016b. doi: 10.1051/0004-6361/201527728.
- Charlotte Götz, Herber Gunell, Martin Volwerk, Arnaud Beth, Anders Eriksson, Marina Galand, Pierre Henri, Hans Nilsson, Cyril Simon Wedlund, Markku Alho, Laila Andersson, Nicolas Andre, Johan De Keyser, Jan Deca, Yasong Ge, Karl-Heinz Glaßmeier, Rajkumar Hajra, Tomas Karlsson, Satoshi Kasahara, Ivana Kolmasova, Kristie LLera, Hadi Madanian, Ingrid Mann, Christian Mazelle, Elias Odelstad, Ferdinand Plaschke, Martin Rubin, Beatriz Sanchez-Cano, Colin Snodgrass, and Erik Vigren. Cometary Plasma Science – A White Paper in response to the Voyage 2050 Call by the European Space Agency. *arXiv e-prints*, art. arXiv:1908.00377, Aug 2019.
- Herbert Gunell, Charlotte Goetz, Cyril Simon Wedlund, Jesper Lindkvist, Maria Hamrin, Hans Nilsson, Kristie LLera, Anders Eriksson, and Mats Holmström. The infant bow shock: a new frontier at a weak activity comet. *A&A*, 619:L2, November 2018. doi: 10.1051/0004-6361/201834225.
- F. L. Johansson, A. I. Eriksson, N. Gilet, P. Henri, G. Wattieaux, M. G. G. T. Taylor, C. Imhof, and F. Cipriani. A charging model for the Rosetta spacecraft. *A&A*, 642:A43, October 2020. doi: 10.1051/0004-6361/202038592.
- R. L. Kessel, A. J. Coates, U. Motschmann, and F. M. Neubauer. Shock normal determination for multiple-ion shocks. *J. Geophys. Res.*, 99(A10):19359–19374, October 1994. doi: 10.1029/94JA01234.
- C. Koenders, K.-H. Glassmeier, I. Richter, U. Motschmann, and M. Rubin. Revisiting cometary bow shock positions. *Planetary and Space Science*, 87:85–95, October 2013. doi: 10.1016/j.pss.2013.08.009.
- K. E. Mandt, A. Eriksson, N. J. T. Edberg, C. Koenders, T. Broiles, S. A. Fuselier, P. Henri, Z. Nemeth, M. Alho, N. Biver, A. Beth, J. Burch, C. Carr, K. Chae, A. J. Coates, E. Cupido, M. Galand, K.-H. Glassmeier, C. Goetz, R. Goldstein, K. C. Hansen, J. Haiducek, E. Kallio, J.-P. Lebreton, A. Luspay-Kuti, P. Mokashi, H. Nilsson, A. Opitz, I. Richter, M. Samara, K. Szego, C.-Y. Tzou, M. Volwerk, C. Simon Wedlund, and G. Stenberg Wieser. RPC observation of the development and evolution of plasma interaction boundaries at 67P/Churyumov-Gerasimenko. *MNRAS*, 462:S9–S22, November 2016. doi: 10.1093/mnras/stw1736.
- F. M. Neubauer, K. H. Glassmeier, M. Pohl, J. Raeder, M. H. Acuña, L. F. Burlaga, N. F. Ness, G. Musmann, F. Mariani, M. K. Wallis, E. Ungstrup, and H. U. Schmidt. First results from the Giotto magnetometer experiment at comet Halley. *Nature*, 321:352–355, May 1986. doi: 10.1038/321352a0.
- H. Nilsson, G. Stenberg Wieser, E. Behar, H. Gunell, M. Galand, C. Simon Wedlund, M. Alho, C. Goetz, M. Yamauchi, P. Henri, and E. Odelstad A.I. Eriksson. Evolution of the ion environment of comet 67P during the rosetta mission as seen by RPC-ICA. *Monthly Notices of the Royal Astronomical Society*, 469 (Suppl.2):S252–S261, 2017. doi: 10.1093/mnras/stx1491.
- N. Omid and D. Winske. A kinetic study of solar wind mass loading and cometary bow shocks. *J. Geophys. Res.*, 92(A12):13409–13426, December 1987. doi: 10.1029/JA092iA12p13409.
- C. Simon Wedlund, E. Behar, H. Nilsson, M. Alho, E. Kallio, H. Gunell, D. Bodewits, K. Heritier, M. Galand, A. Beth, M. Rubin, K. Altwegg, M. Volwerk, G. Gronoff, and R. Hoekstra. Solar wind charge exchange in cometary atmospheres III. Results from the Rosetta mission to comet 67P/Churyumov-Gerasimenko. *Astronomy & Astrophysics*, 2019. doi: 10.1051/0004-6361/201834881.
- Edward J. Smith, Bruce T. Tsurutani, James A. Slavin, Douglas E. Jones, George L. Siscoe, and D. Asoka Mendis. International cometary explorer encounter with Giacobini-Zinner: Magnetic field observations. *Science*, 232(4748):382–385, 1986. ISSN 0036-8075. doi: 10.1126/science.232.4748.382.

A Additional events

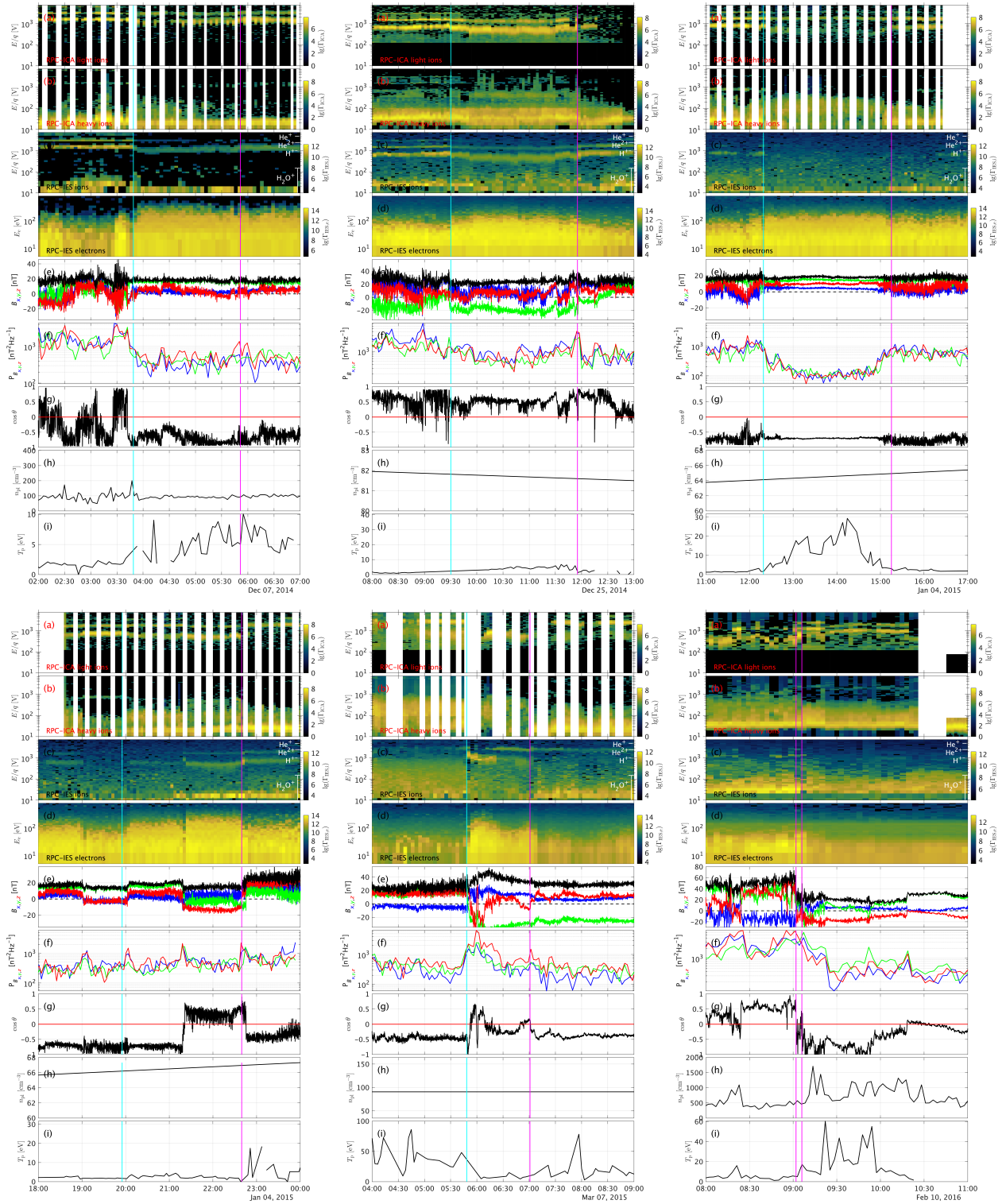


Figure 6: Observations of the plasma for the events shown in Table 1. Format is the same as in Figure 1.

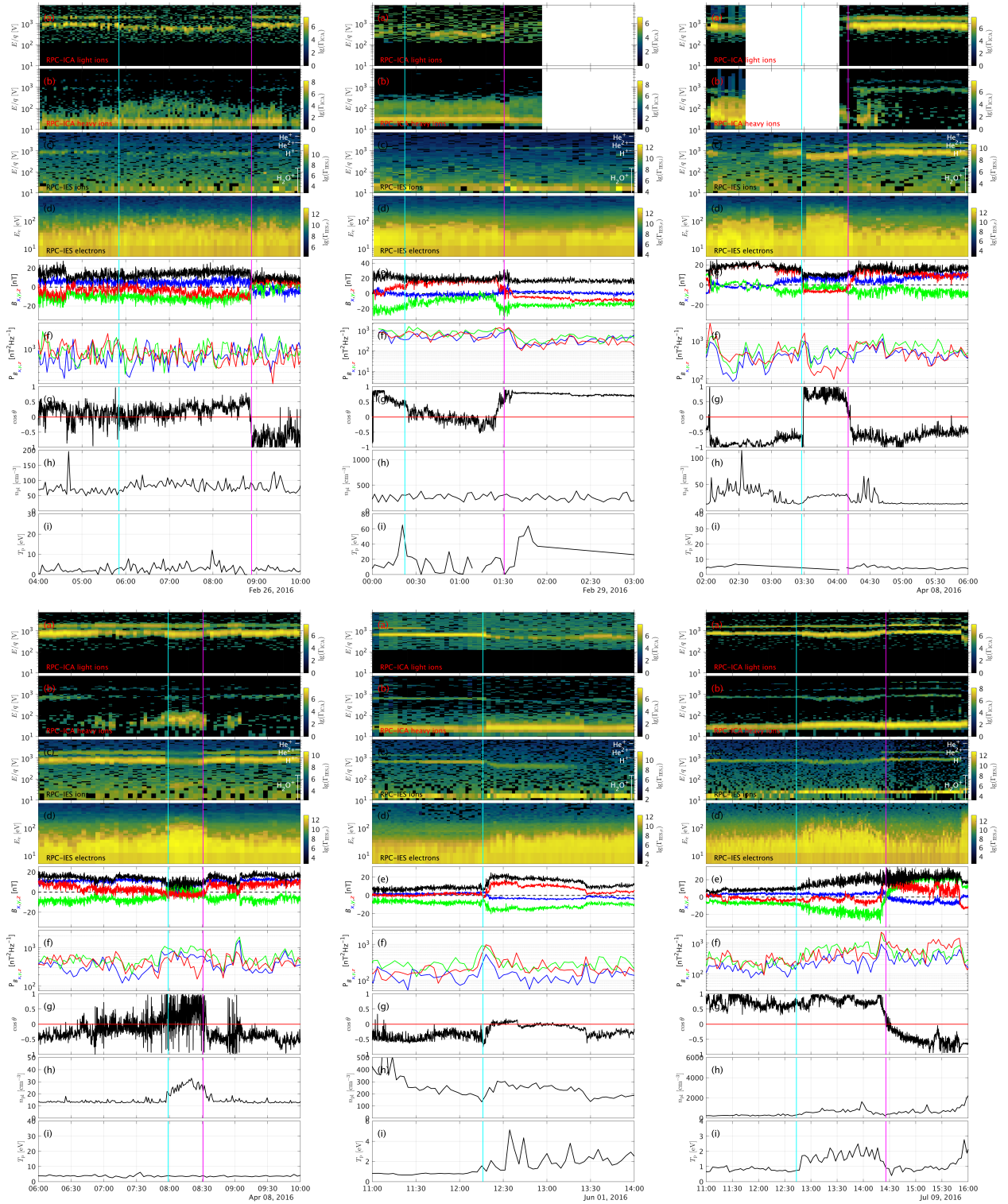


Figure 7: Observations of the plasma for the events shown in Table 1. Format is the same as in Figure 1.